arXiv:1303.6297v1 [cond-mat.str-el] 25 Mar 2013

Tetramerization in a SU(4)-Heisenberg model on the honeycomb lattice

Miklós Lajkó[1,2] and Karlo Penc[1,2]

[1]Institute for Solid State Physics and Optics, Wigner Research Centre for Physics,
Hungarian Academy of Sciences, H-1525 Budapest, P.O.B. 49, Hungary
[2]Department of Physics, Budapest University of Technology and Economics, 1111 Budapest, Hungary

(Dated: March 27, 2013)

The SU(4) Heisenberg model can serve as a low energy model of the Mott insulating state in materials where the spins and orbitals are highly symmetric, or in systems of alkaline-earth atoms on optical lattice. Recently, it has been argued that on the honeycomb lattice the model exhibits a unique spin-orbital liquid phase with an algebraic decay of correlations [P. Corboz *et al.*, Phys. Rev. X **2**, 041013 (2012)]. Here we study the instability of the algebraic spin-orbital liquid toward spontaneous formation of SU(4) singlet plaquettes (tetramerization). Using a variational Monte Carlo approach to evaluate the projected wave-function of fermions with π-flux state, we find that the algebraic liquid is robust, and that a finite value of the next nearest exchange is needed to induce tetramerization. We also studied the phase diagram of a model which interpolates between the nearest neighbor Heisenberg model and a Hamiltonian for which the singlet-plaquette product state is an exact ground state.

PACS numbers: 67.85.-d, 71.10.Fd, 75.10.Jm,75.10.Kt

I. INTRODUCTION

In transition metal oxides the partially filled d-orbitals usually undergo a Jahn-Teller distortion which removes the orbital degeneracy. However, in certain cases the orbitals remain fluctuating down to low temperatures at energies comparable to those of spin fluctuations. Possible examples include the triangular system $\mathrm{LiNiO_2}$ [1, 2], and more recently $\mathrm{Ba_3CuSb_2O_9}$ [3, 4] with Cu ions forming a decorated honeycomb lattice. Theoretically, the scenario of spin-orbital liquids was studied in Refs. [5–12].

The minimal model which includes the interaction of spins and orbitals is the Kugel-Khomskii model. Due to the spatial extension of the orbitals, the Kugel-Khomskii model is usually anisotropic in the orbital part. However, under specific circumstances, the model acquires its highest symmetry form and can be written as

$$\mathcal{H} = \sum_{\langle i,j\rangle} \left(2\mathbf{S}_i \cdot \mathbf{S}_j + \frac{1}{2}\right)\left(2\mathbf{T}_i \cdot \mathbf{T}_j + \frac{1}{2}\right) , \tag{1}$$

where $\mathbf{S}_i$ are spin-1/2 operators acting on the $|\uparrow\rangle$ and $|\downarrow\rangle$ states and $\mathbf{T}_j$ are operators acting on the twofold degenerate orbital degrees of freedom (which we denote by a and b). For this special case the system is fully SU(4) symmetric. Denoting the local spin-orbital states by colors, |🔴⟩ $=|\uparrow a\rangle$, |🟢⟩ $=|\downarrow a\rangle$, |🔵⟩ $=|\uparrow b\rangle$, and |🟡⟩ $=|\downarrow b\rangle$, the Hamiltonian (1) is equivalent to

$$\mathcal{H} = \sum_{\langle i,j\rangle} P_{i,j} , \tag{2}$$

where $P_{i,j}$, acting in the color space, interchanges the states on sites i and j. This Hamiltonian defines the SU(4) symmetric Heisenberg model.

The same model also arises in the Mott insulating state of ultra-cold alkaline-earth atoms trapped in an optical lattice. In this case, it is the nuclear spin of length F which becomes the only relevant degree of freedom with $N = 2F + 1$ states, and the interaction leads to the SU(N) symmetric Heisenberg model[13–16].

The absence of spin and orbital ordering in $\mathrm{Ba_3CuSb_2O_9}$ [3, 4] prompted authors of Ref. [17] (including the present authors) to study the symmetric Kugel-Khomskii model on the honeycomb lattice. Combining the results of a variety of numerical and analytical methods, they proposed that an algebraic spin-orbital liquid (or color liquid) state is realized. In this color-liquid the color-color correlation decays algebraically with the distance, and the ground state does not break any space group symmetry, nor the SU(4) symmetry. In particular, it can be described by a Gutzwiller projected variational wave function based on the π-flux state of fermions on the honeycomb lattice at 1/4 filling. In the π-flux state a gauge field corresponding to a magnetic flux of half the flux quantum is introduced. The Fermi surface is actually a point, as the Fermi-level is at the Dirac point introduced by the π-flux. Naturally, the question arises if the variational state is stable against the opening of a gap at the Fermi level of the unprojected fermions. This can be realized by modulating the hoppings and the on-site energies. Here, our aim is to study the stability of the algebraic color liquid state against such an instability, the tetramerization, using the variational approach.

The motivation behind choosing tetramerization is not only because it opens a gap in the unprojected fermion spectrum, but also by the natural tendency of the SU(4) colors to form 4-site singlet plaquettes [7]. Such plaquettes were observed *e.g.* in two-leg SU(4) ladders [18], and even a Hamiltonian based on projection operators can be constructed where decoupled SU(4) singlet plaquettes are the exact ground state [19]. Tetramerization also happens in two-dimensional models: on the checkerboard lattice the plaquette-product wave function is an exact ground state of a suitable Hamiltonian which is a sum of projectors, and the singlet formation persist also in the simple Heisenberg model [20]. For the square lattice, the situation is less evident: plaquette formation was proposed in Refs. [21–23], but debated in Ref. [10]. Our current understanding is that a dimerization occurs [24].

The paper is structured as follows: In Sec. II we construct a Hamiltonian which has singlet-product states as exact ground states. In Sec. III we construct an order parameter to detect tetramerization. In Sec. IV we present results of the variational Monte Carlo calculations. Finally we conclude in Sec. V.

II. A MODEL WITH AN EXACT, TETRAMERIZED GROUND STATE

Using projection operators, we can construct a Hamiltonian for which a singlet-product wave function is an exact ground state, where the four spins of the SU(4) singlets are located on 4-site stars (a central site with the 3 nearest neigbor sites). There are four such equivalent coverings, that are related by translations and inversion. For that reason, we consider the

$$Q_{(ij),(kl)} = \frac{1}{4}(1+P_{ij})(1+P_{kl}) \tag{3}$$

operator, where P_{ij} is the SU(4) symmetric Heisenberg exchange. For disjunct (ij) and (kl) the $Q_{(ij),(kl)} = Q^2_{(ij),(kl)}$ holds, so the $Q_{(ij),(kl)}$ is a projection operator with eigenvalues 0 and 1. It gives 0 if the wave function on the (ij) or the (kl) bonds is antisymmetric, *i.e.* belongs to a singlet. If we choose the (ij) and (kl) bonds to be the nearest neighbor parallel bonds, as shown in Fig. 1(a), at least one of the (ij) and (kl) bonds is covered by a SU(4) singlet, so that $Q_{(ij),(kl)}|\Psi_{\rm SP}\rangle = 0$ for any of the four $|\Psi_{\rm SP}\rangle$'s. It follows, that the $|\Psi_{\rm SP}\rangle$ are ground states of the

$$\mathcal{H}_Q = \sum_{(ij),(kl)} Q_{(ij),(kl)} \tag{4}$$

Hamiltonian with 0 energy: since it is a sum of positive definite operators, the energy of the ground state must be ≥ 0. The sum in the $\mathcal{H}_Q$ is over the $3N$ nearest neighbor parallel bond configuration. We note that this construction is slightly different from those mentioned in Refs. [19, 25, 26].

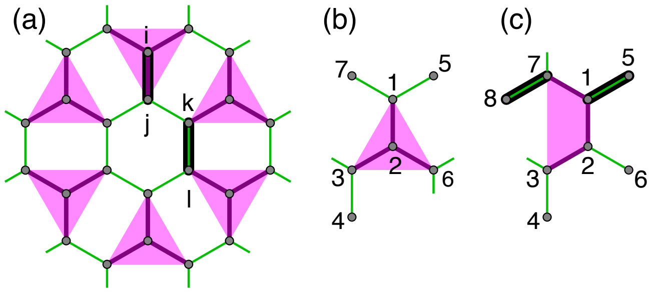

FIG. 1. (Color online) (a) The modulation of the bond energies in the tetramerized state on the honeycomb lattice. In the ground state of the $\mathcal{H}_Q$ the spins on the four sites connected by the purple bonds make a SU(4) singlet (here emphasized by the magenta triangles), these singlet tetramers are decoupled from each other. The two thick black bonds represent the configuration of the (ij) and (kl) bonds of the $Q_{(ij),(kl)}$ projector in the $\mathcal{H}_Q$ Hamiltonian. (b) A SU(4) spin singlet that is an eigenstate of the Q projection operators with 0 eigenvalue. (c) An invalid SU(4) singlet, as the $Q_{(15)(78)}$ cannot be satisfied.

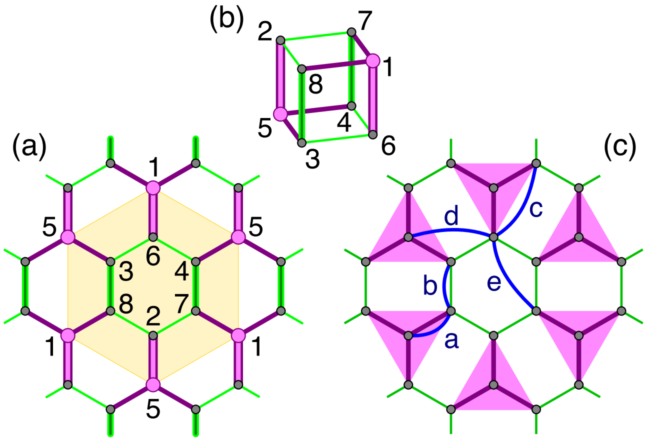

FIG. 2. (Color online) Graphical representation of the $R_{yz} = P_{1,6} + P_{2,5} - P_{3,8} - P_{4,7}$ component of the three-dimensional order parameter: (a) on the lattice (the numbers enumerate equivalent sites in the 8-site unit cell), and (b) in the cube. The cube is topologically equivalent to ordering in the 8-site unit cell. The bonds participating on R_{xy} are shown as double lines. We have assumed that one of out of the four tetramerized ground state is realized, in this case $(R_x, R_y, R_z) \propto (1,1,1)$. (c) The non-equivalent nearest neighbor and next nearest neighbor bond energies in the tetramerized state. In the singlet-product wave functions the $\langle P_a\rangle = \langle P_c\rangle = -1$ and $\langle P_b\rangle = \langle P_d\rangle = \langle P_e\rangle = 1/4$, while in the absence of tetramerization $\langle P_a\rangle = \langle P_b\rangle = \langle P_1\rangle$ and $\langle P_c\rangle = \langle P_d\rangle = \langle P_e\rangle = \langle P_2\rangle$.

We can also easily convince ourselves that no other type of SU(4) singlet coverings satisfies $\mathcal{H}_Q$. Here we follow the site numbering shown in Fig. 1: (i) To make $Q_{(12)(34)}$ satisfied, we choose to antisymmetrize the spins on bond (12); (ii) To satisfy $Q_{(15)(23)}$, we antisymmetrize (23); (iii) To make the $Q_{(17)(26)}$ happy, we need to choose to antysimmetrize spins on band (26) [as shown in Fig. 1(b)]. Antisymmetrizing (17) would mean that we are not able to satisfy $Q_{(15)(78)}$ Fig. 1(c), as we cannot antisymmetrize colors on more than four sites. So, the star shaped singlet in Fig. 1(b) is the only possible SU(4) singlet that satisfies all the $Q_{(ij)(kl)}$. The two choices we made in step (i) and (ii) in selecting the bonds of Q on which we antisymmetrized the spin lead to the fourfold degeneracy of the ground state.

The following model interpolates between the Heisenberg model and the $\mathcal{H}_Q$:

$$\mathcal{H}_\alpha = \sum_{(ij)} P_{ij} + \frac{\eta}{4} \sum_{(ij),(kl)} \left(1 + P_{ij}P_{kl}\right) . \tag{5}$$

For $\eta = 1$, the $\mathcal{H}_\eta = \mathcal{H}_Q$, while for $\eta = 0$ we recover the nearest neighbor SU(4) Heisenberg model, Eq. (2). To find the transition point between these two cases, we will study this model using the VMC approach in Sec. IV.

III. TETRAMERIZATION ORDER PARAMETER

To construct the order parameter of the tetramerization, we start from the 8 site unit cell of the tetramerized state shown in Fig. 2(a). The connectivity of the sites in the unit cell is topologically equivalent to a cube, so the O_h point group of the cube can be used to obtain the order parameter. The expectation values of the $P_{i,j}$ exchange operators on the 12 nearest neighbor bonds in the unit cell transform according to the A_{1g}, E_{g}, T_{2g}, T_{1u}, and T_{2u} irreducible representations of the O_h group, and can serve to detect order of some kind. The order parameter of the tetramerization is given by

$$\mathbf{R} = \begin{pmatrix} P_{1,6} + P_{2,5} - P_{3,8} - P_{4,7} \\ P_{1,7} - P_{2,8} + P_{3,5} - P_{4,6} \\ P_{1,8} - P_{2,7} - P_{3,6} + P_{4,5} \end{pmatrix}, \tag{6}$$

and transforms as the three dimensional T_{2g} irreducible representation. For the singlet product ground state of the $\mathcal{H}_Q$ shown in Fig. 2(a) $\mathbf{R} = (-5/2, -5/2, -5/2)$, while the for the remaining three ground states $\mathbf{R} = (-5/2, 5/2, 5/2)$, $\mathbf{R} = (5/2, -5/2, 5/2)$, and $\mathbf{R} = (5/2, 5/2, -5/2)$. Denoting the components of the order parameter as $\mathbf{R} = (R_{yz}, R_{xz}, R_{xy})$ [we use the (yz, xz, xy) notation as it also transforms according to the T_{2g} irreducible representation in O_h], the Landau free energy can be written as

$$E = -c_2\left(R_{yz}^2 + R_{xz}^2 + R_{xy}^2\right) + c_3 R_{yz} R_{xz} R_{xy} + \cdots \tag{7}$$

The cubic invariant with $c_3 > 0$ selects the 4 directions [$R \propto (-1, -1, -1)$, $(-1, 1, 1)$, $(1, -1, 1)$, and $(1, 1, -1)$], and makes the phase transition into the tetramerized phase a first order one.

In the variational calculation, where we explicitly break the four-fold degeneracy by hand, it is sufficient to consider the difference of the energies on a nearest neighbor bond belonging to a tetramer and on a nearest neighbor bond connecting two tetramers [see Fig. 2(c)]:

$$r = -\frac{4}{5}\left(\langle P_a \rangle - \langle P_b \rangle\right) . \tag{8}$$

For the uniform spin-orbital liquid that does not break the space group of the lattice $r = 0$, while for the fully tetramerized state $\langle P_a \rangle = -1$ and $\langle P_b \rangle = 1/4$, so that $r = 1$ in this case. The two order parameters are related as $\mathbf{R} = 2(\langle P_a \rangle - \langle P_b \rangle)(1, 1, 1) = -(5r/2)(1, 1, 1)$.

IV. VARIATIONAL MONTE CARLO RESULTS

The variational approach is based on the fermionic representation of the SU(N) algebra. The exchange operator $P_{i,j}$ can be written as

$$P_{i,j} = -\sum_{\alpha,\beta=1}^{N} f_\alpha^\dagger(i) f_\beta^\dagger(j) f_\beta(i) f_\alpha(j) , \tag{9}$$

where $f_\alpha^\dagger(i)$ creates a fermion of color α on site i, and $f_\alpha(i)$ annihilates it. To treat the four fermion term, it is customary to introduce a bond mean-field decoupling of the $P_{i,j}$ [27], leading to a free-fermion Hamiltonian, where the hopping amplitudes are determined self-consistently. The mean-field procedure often results in solutions where the product of the hoppings around a plaquette is a complex number $\propto e^{i\Phi}$, as if the fermions were picking up a phase due to a magnetic field with flux Φ threading through the plaquette (in convenient units). The finite flux can considerably change the band structure. Chiral solutions (with $\Phi \neq 0, \pi$) were found for the SU(N) model with $N \geq 5$ on the square lattice [28] and for the SU(6) model on the honeycomb lattice [29]. While the mean-field solutions give a very useful insight into the possible nature of the ground state, it describes free fermions where the on-site occupancy is fixed on the average only.

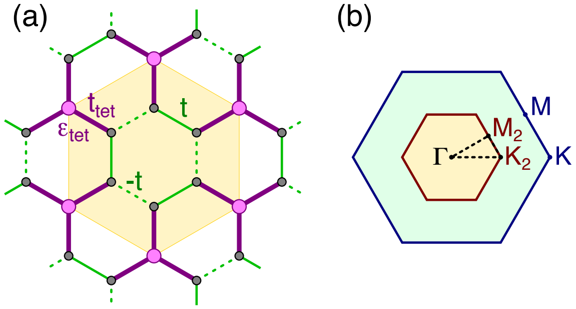

FIG. 3. (Color online) (a) The modulation of the hopping amplitudes and of the on-site energies in the π-flux hopping Hamiltonian. The dashed hoppings represent negative hopping amplitudes. The 8-site hexagonal unit cell is shown in orange. (b) The Brillouin zone of the honeycomb lattice (blue, with high symmetry points K and M) and of the 8-site unit cell (red, with high symmetry points K_2 and M_2)

In a complementary approach one does not search for mean-field solutions, but takes the ground state wave function of some free-fermion Hamiltonian, and by applying a Gutzwiller projection one ensures that the occupation of each site is exactly one. The projection is done numerically on a finite size cluster, using Monte-Carlo importance sampling, where one can efficiently sample the wave function and calculate the energy and correlations [30, 31]. Regarding two-dimensional SU(N) Heisenberg models, the method has been applied to the SU(4) model on the square [10] and honeycomb lattice [17], and to the SU(3) model on the triangular lattice [32] and honeycomb lattice [33].

As already mentioned in the introduction, the energy of the Gutzwiller projected π-flux state is much lower than the energy of the 0-flux state for the SU(4) model on the honeycomb lattice [17]. So to study tetramerization within the variational approach, we modify the free fermion Hamiltonian by strengthening the hoppings t_tet on the bonds belonging to the tetramers and by introducing a negative onsite energy ε_tet for the sites at the center of the tetramers, while maintaining the π-flux state. The Hamiltonian is given by

$$\mathcal{H}_f = \sum_{\alpha=1}^{4}\left[\sum_i \varepsilon_i f_{i,\alpha}^\dagger f_{i,\alpha} - \sum_{\langle i,j\rangle} t_{i,j}\left(f_{j,\alpha}^\dagger f_{i,\alpha} + f_{i,\alpha}^\dagger f_{j,\alpha}\right)\right] , \tag{10}$$

the $t_{i,j}$ hoppings and ε_i on-site energies are chosen as shown in Fig. 3(a). The sign of the $t_{i,j}$ is such that the product of the hoppings around the hexagons is negative: the product is either $-t^6$ or $-t^2 t_\text{tet}^4$, depending on the hexagon. This realizes the π-flux state, the variational state with the lowest energy for the nearest neighbor exchange.

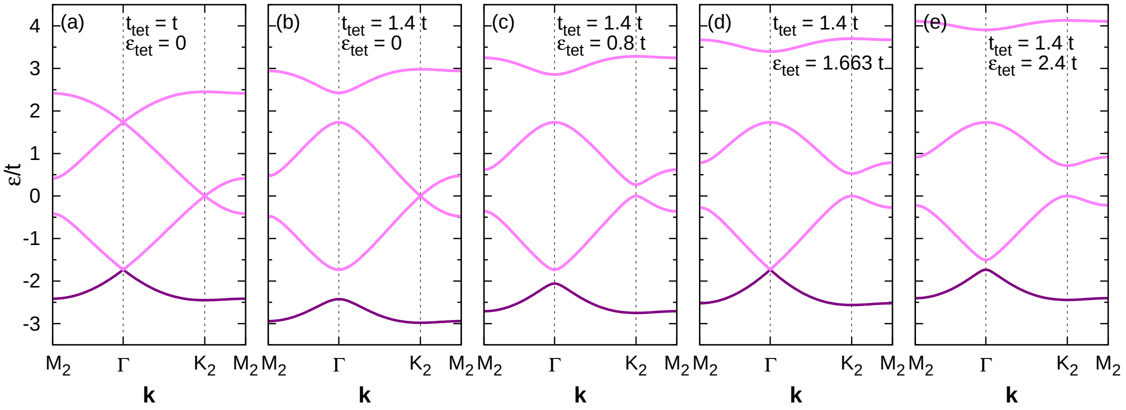

FIG. 4. (Color online) The two-fold degenerate bands of the free fermions of the tetramerized π-flux state for a few selected values of the ε_{tet} and t_{tet} along a path connecting high-symmetry points in the reduced Brillouin zone [see Fig. 3(b)]. Γ is the center of the Brillouin-zone ($\mathbf{k} = 0$), M_2 is the $\mathbf{k} = (\pi/3, 0)$ (and the symmetry related points), and K_2 is the $\mathbf{k} = (0, 2\pi/3\sqrt{3})$. Occupied bands are colored dark purple, while empty bands are colored light purple.

A. Free fermions in the *k*-space

Before discussing the results of the Gutzwiller projection, it is instructive to look at the properties of free fermions with π-flux per plaquette. Fourier transforming the fermionic operators in a conveniently chosen gauge, we can write the hopping hamiltonian in the k-space as an 8×8 matrix of the form (following the site ordering shown in Fig. 2)

$$\mathcal{H}_f(\mathbf{k}) = \begin{pmatrix} \mathcal{E} & -\mathcal{F} \\ -\mathcal{F}^\dagger & \mathcal{E} \end{pmatrix} , \tag{11}$$

where the only nonzero element of $\mathcal{E}$ matrix is $\mathcal{E}_{1,1} = \varepsilon_{\text{tet}}$ and

$$\mathcal{F} = \begin{pmatrix} 0 & e^{2ik_y} t_{\text{tet}} & e^{i\sqrt{3}k_x - ik_y} t_{\text{tet}} & e^{-i\sqrt{3}k_x - ik_y} t_{\text{tet}} \\ e^{2ik_y} t_{\text{tet}} & 0 & t & -t \\ e^{i\sqrt{3}k_x - ik_y} t_{\text{tet}} & -t & 0 & t \\ e^{-i\sqrt{3}k_x - ik_y} t_{\text{tet}} & t & -t & 0 \end{pmatrix} \tag{12}$$

describes the hopping between the nearest neighbor sites. In the absence of the on-site potential ε_{tet}, the $\mathcal{E} = 0$ and by squaring the eigenvalue problem we get $\mathcal{F}^\dagger\mathcal{F}|\psi\rangle = \varepsilon^2|\psi\rangle$, *i.e.* the bands are particle-hole symmetric.

Solving for the eigenvalues of Eq. (11), we find four two-fold degenerate bands in the Brillouin zone of the 8-site unit cell, shown in Fig. 4. The two-fold degeneracy is the direct consequence of the π-flux. In the limiting case of $t_{\text{tet}} = 0$, when we end up with a hexagon and two isolated sites in the unit cell, the degeneracy is present as the alternating t hoppings on the hexagon makes the energy levels double degenerate. In the other limit, when $t = 0$, the situation is simpler, as there are two decoupled tetramers in the unit cell, trivially giving a two-fold degeneracy. To see the degeneracy for arbitrary values of hopping parameters, we start from a one-fermion wave function $|\psi_{1A}\rangle$, where the amplitude is 1 at the center of one of the tetramers. We can then generate a four-dimensional Hilbert-space by successively acting with the $\mathcal{H}_f(\mathbf{k})$ to the $|\psi_{1A}\rangle$ state:

$$|\psi_{1A}\rangle = (0, 0, 0, 0, 1, 0, 0, 0) , \tag{13}$$

$$|\psi_{2A}\rangle = \frac{1}{\sqrt{3}} (0, 1, 1, 1, 0, 0, 0, 0) , \tag{14}$$

$$|\psi_{3A}\rangle = \frac{1}{3\sqrt{1 - |\gamma_\mathbf{k}|^2}} \Big(0, e^{2ik_y} - \gamma^*_\mathbf{k}, e^{i\sqrt{3}k_x - ik_y} - \gamma^*_\mathbf{k}, e^{-ik_y - i\sqrt{3}k_x} - \gamma^*_\mathbf{k}, 0, 0, 0, 0\Big) , \tag{15}$$

$$|\psi_{4A}\rangle = \frac{1}{\sqrt{27}\sqrt{1 - |\gamma_\mathbf{k}|^2}} \Big(0, 0, 0, 0, 0, e^{-i\sqrt{3}k_x - ik_y} - e^{i\sqrt{3}k_x - ik_y}, e^{2ik_y} - e^{-i\sqrt{3}k_x - ik_y}, e^{i\sqrt{3}k_x - ik_y} - e^{2ik_y}\Big) , \tag{16}$$

where

$$\gamma_\mathbf{k} = \frac{1}{3}\left(e^{-i\sqrt{3}k_x + ik_y} + e^{i\sqrt{3}k_x + ik_y} + e^{-2ik_y}\right) . \tag{17}$$

Further acting with $\mathcal{H}_f(\mathbf{k})$ on $|\psi_{4A}\rangle$ will result a linear combination of $|\psi_{1A}\rangle$, $|\psi_{2A}\rangle$, $|\psi_{3A}\rangle$, and $|\psi_{4A}\rangle$, so that the Hilbert space closes. In this Hilbert space the hopping Hamiltonian is reduced to

$$\mathcal{H}'_f = -\begin{pmatrix} -\varepsilon_{\text{tet}} & \sqrt{3}\gamma^*_\mathbf{k} t_{\text{tet}} & \sqrt{3(1 - |\gamma_\mathbf{k}|^2)}\, t_{\text{tet}} & 0 \\ \sqrt{3}\gamma_\mathbf{k} t_{\text{tet}} & 0 & 0 & 0 \\ \sqrt{3(1 - |\gamma_\mathbf{k}|^2)}\, t_{\text{tet}} & 0 & 0 & \sqrt{3}t \\ 0 & 0 & \sqrt{3}t & 0 \end{pmatrix} . \tag{18}$$

The dispersion $\varepsilon_\mathbf{k}$ of the fermions is given by the characteristic polynomial of $\mathcal{H}'_f$

$$0 = \varepsilon^4_\mathbf{k} - \varepsilon_{\text{tet}}\varepsilon^3_\mathbf{k} - 3\varepsilon^2_\mathbf{k}\left(t^2 + t^2_{\text{tet}}\right) + 3\varepsilon_{\text{tet}}\varepsilon_\mathbf{k} t^2 + 9|\gamma_\mathbf{k}|^2 t^2 t^2_{\text{tet}} . \tag{19}$$

Similarly, we can start with $|\psi_{1B}\rangle$, where the amplitude is 1 at site 1. This leads to an four-dimensional Hilbert space that is orthogonal to the $\{|\psi_{1A}\rangle, |\psi_{2A}\rangle, |\psi_{3A}\rangle, |\psi_{4A}\rangle\}$, and we end up with a reduced hopping matrix that is the complex conjugate of $\mathcal{H}'_f$, with a spectrum also given by Eq. (19). So we have succesfully block diagonalized $\mathcal{H}_f$ and shown that the spectrum is two-fold degenerate.

In Fig. 4 we show the band structure for different choices of the t_{tet} and ε_{tet}. The bands of the uniform π-flux state of the algebraic color liquid are shown in Fig. 4(a). There are three Dirac-points in the band structure, two at Γ point with $\varepsilon = \pm\sqrt{3}t$ and one at the M_2 point with $\varepsilon = 0$ - the latter one is counterpart of the Dirac-point of the hopping hamiltonian with uniform hoppings, and remains a Dirac point as long as $\varepsilon_{\text{tet}} = 0$, as seen in Fig. 4(b). For the SU(4) problem, however, the lower Dirac-point at $\mathbf{k} = 0$ is more important: it makes the Fermi surface of the quarter filled Fermi sea point-like and is responsible for the algebraic decay of the color-color correlation functions. Tetramerization removes the Dirac point and a gap opens between the lowest band and the band above it at the Γ point. However, fine tuning the parameters, we can recover the Dirac point: for $\mathbf{k} = 0$ the Eq. (19) factorizes into $(\varepsilon_{\mathbf{k}}^2 - 3t^2)(\varepsilon_{\mathbf{k}}^2 - \varepsilon_{\text{tet}}\varepsilon_{\mathbf{k}} - 3t_{\text{tet}}^2) = 0$. As we change the ε_{tet} and t_{tet}, a level crossing happens (i.e. the gap closes) at $\varepsilon = -\sqrt{3}t$ when

$$\varepsilon_{\text{tet}} = \frac{\sqrt{3}}{t}\left(t_{\text{tet}}^2 - t^2\right) . \tag{20}$$

A typical spectrum with a Dirac-point for such a particular value of ε_{tet} is shown in Fig. 4(d). We note that in a finite size cluster a level crossing happens in the free-fermion spectrum at the Γ point.

B. Gutzwiller projection

In the following, we calculate the expectation value of the exchange Hamiltonian in the Gutzwiller projected wave function using Monte-Carlo importance sampling as we change the values of t_{tet} and ε_{tet} in the π-flux phase. A short description of the method we use is given in Ref. [17]. We choose a 96 site cluster that has the full symmetry of the hexagonal lattice and is compatible with the tetramerization pattern. In our Monte-Carlo algorhythm an elementary update was the exchange of two randomly chosen fermions at arbitrary sites with different colors. Each run had 10^{10} elementary updates. To avoid any autocorrelation effect, we performed measurements after every 1000 updates, the distance that corresponds to around 5 times the autocorrelation length. We averaged over all the bonds when calculating the energy, and the errors of the energy/site values are of the order of 10^{-4}, thus much smaller than the symbol sizes on the plots. Furthermore, the boundary conditions (periodic or antiperiodic) of the hopping hamiltonian were chosen so that to avoid the degeneracy of the free-fermion ground state.

1. *Stability of the Algebraic color liquid*

First, we consider the stability of the algebraic color liquid against tetramerization. For that reason we vary the t_{tet} and ε_{tet} in a systematic way and measure the expectation value of the energy and the tetramerization order parameter, [Eq. (8)]. The energy per site is given by

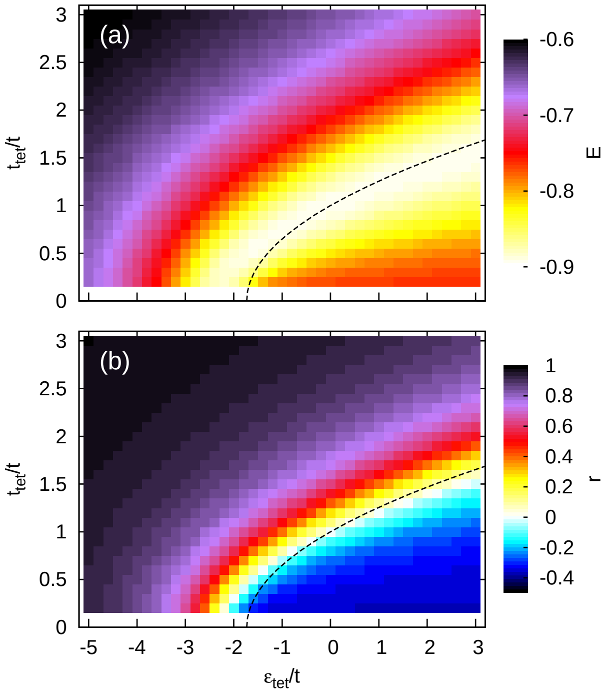

FIG. 5. (Color online) (a) The energy of the SU(4) nearest neighbor Heisenberg model and (b) the order parameter r in the Gutzwiller projected variational wave function as a function of the t_{tet} and ε_{tet} parameters of the hopping Hamiltonian, calculated on a 96 site cluster. The t_{tet} and ε_{tet} were varied in steps of $0.1t$ and $0.2t$, respectively. Along the dashed black line the free fermion Fermi surface becomes a point, following the condition given by Eq. (20). The energy minima closely follows that line, and similarly the order parameter vanishes in the vicinity of that line.

$$E = \frac{3}{2}\frac{\langle P_a\rangle + \langle P_b\rangle}{2} , \tag{21}$$

where $\langle P_a\rangle$ and $\langle P_b\rangle$ are the expectation value of the exchange on the intra- and inter-tetramer bonds, respectively [Fig. 2(c)]. Results for the energy as a function of the t_{tet} and ε_{tet} are shown in Fig. 5(a), together with the tetramerization parameter, Fig. 5(b). It appears that the energy is minimal in a valley roughly following the condition (20), that is required for the Dirac points to form at the Fermi surface, and at the same time the tetramerization order parameter disappears. The actual minimum is realized for the $t_{\text{tet}} = t$ and $\varepsilon_{\text{tet}} = 0$: The π-flux state is stable against tetramerization for the nearest neighbor exchange on the Heisenberg lattice. This is explicitly seen in Fig. 6(a), where the energy and order parameter values of Fig. 5 are replotted with t_{tet} and ε_{tet} being implicit variables. Quite surprisingly, the tuning of the parameters t_{tet} and ε_{tet} in the free fermion Hamiltonian may have similar effects after the Gutzwiller projection. Namely, even for quite

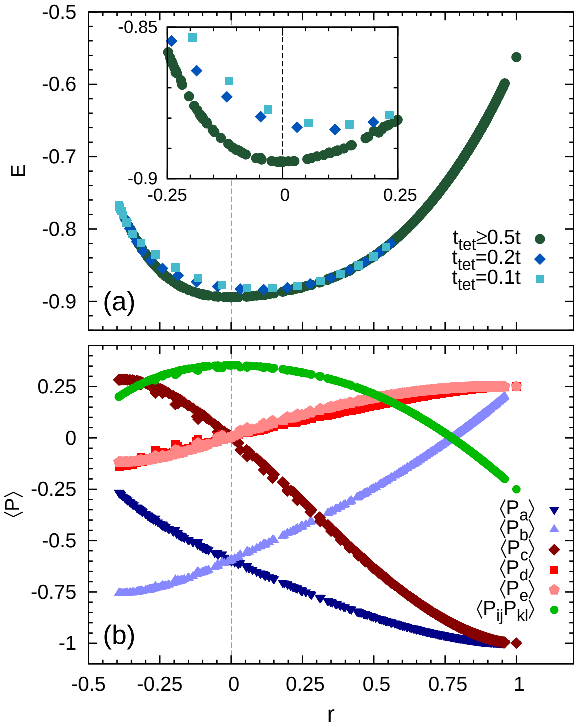

FIG. 6. (Color online) (a) Energy per site of the nearest neighbor model, Eq. (21), as a function of the tetramerization parameter r, Eq. (8), for various t_{tet} and ε_{tet} values. The singlet product wave function is the maximally tetramerized state with $r = 1$ and $E = -9/16$ (the rightmost points in the plot). The plot around the $r = 0$ is enlarged in the inset. (b) The expectation values of the exchange operators on the non-equivalent first and second neighbor bonds, and of the four site $P_{ij}P_{kl}$ operator. Statistical error is smaller that the symbol size.

different values of t_{tet} and ε_{tet} the E vs. r plot essentially lay on a single curve. Some deviation from this behavior is seen as $t_{\text{tet}} \to 0$, as exemplified by the $t_{\text{tet}}/t = 0.2$ and 0.4 points for not too large values of $|r|$ (for larger values of $|r|$ the points for these hoppings merge with other points). This behavior is also seen for the exchanges on the different non-equivalent bonds [Fig. 6(b)].

2. Phase transition between the algebraic color liquid and the tetramerized state

For $t = 0$ the free-fermion Hamiltonian describes decoupled tetramers with localized fermions. The lowest energy level of a decoupled star is singly degenerate, and Gutzwiller projecting the four fermions ground state gives an SU(4) siglet. Not surprisingly, the Gutzwiller projected wave function becomes the tetramer-factorized wave function in this case, the exact ground state of the of the Hamiltonian (4). So changing the η in the Hamiltonian (5), we may expect that a phase transition occurs at finite value of the η parameter between the uniform color liquid and the tetramerized state and that the transition can be captured by the variational wave function.

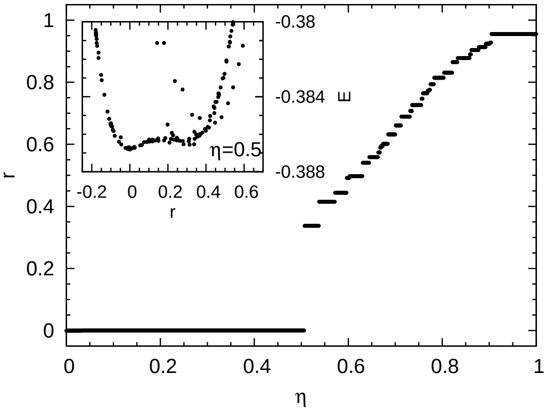

FIG. 7. The tetramerization order parameter r as a function of η in Eq. (5). A first-order phase transition occurs at $\eta \approx 0.5$ between the algebraic color liquid ($r = 0$) and the tetramerized phase ($r > 0$). In the inset we show the expectation value as a function of the order parameter close to the phase transition, at $\eta = 0.5$. Each points corresponds to a different value of the free-fermion parameters t_{tet} and ε_{tet}, as calculated by the Variational Monte Carlo on the 96 site cluster.

To explore this possibility, we have looked up minimum energy solution among the calculated t_{tet} and ε_{tet} values for a given η, and plotted the corresponding value of order parameter r. The energy per site is given by

$$E = \frac{3}{2}\frac{\langle P_a\rangle + \langle P_b\rangle}{2} + \frac{3}{4}\eta\left(1 + \langle P_{ij}P_{kl}\rangle\right) , \tag{22}$$

and the result is shown in Fig. 7. The algebraic color liquid is stable up to $\eta \approx 0.5$, where a first order transition happens into the tetramerized state – this agrees with the existence of the cubic invariant of the order parameter in Eq. (7). The first order nature of the transition is further supported by the energy versus order parameter plot, shown in the inset of Fig. 7 for $\eta = 0.5$: we can clearly recognize the two minima of the energy, one corresponding to the algebraic color liquid ($r = 0$), the other at $r \approx 0.3$ to the tetramerized state. And, as discussed above, for $\eta = 1$, we recover the fully tetramerized ground state with $r = 1$.

3. Tetramerization due to next nearest exchange

Extending the Hamiltonian (2) with the next nearest neighbor exchange J_2, the number of bonds within a singlet tetramer increases [c in Fig. 2(c)], but so does the number of bonds between the singlets [d and e in Fig. 2(c)] as well. The energy per site is now given by

$$E = \frac{3J_1}{2}\frac{\langle P_a\rangle + \langle P_b\rangle}{2} + 3J_2\frac{\langle P_c\rangle + 2\langle P_d\rangle + \langle P_e\rangle}{4} , \tag{23}$$

where J_1 is the nearest neighbor exchange coupling. The answer to the question if the J_2 drives the system toward

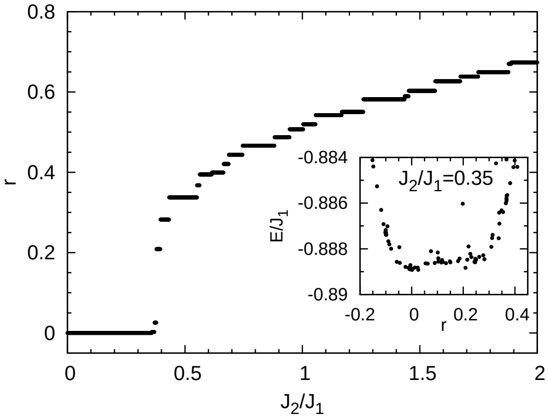

FIG. 8. The tetramerization order parameter as a function of J_2/J_1 in the model with next nearest exchange J_2. A weakly first-order phase transition occurs at $J_2/J_1 \approx 0.38$ between the algebraic color liquid and the tetramerized phase. In the inset the energy vs. order parameter is shown for the calculated t_{tet} and ε_{tet} values close to the transition point.

tetramerization is not evident. In the limiting case of the tetramer-factorized wave function, the expectation value of the energy is $E = -9J_1/16 - 3J_2/16 = -0.5625J_1 - 0.1875J_2$. This energy is to be compared with the expectation value of the energy in the algebraic color liquid, where $\langle P_a \rangle = \langle P_b \rangle \approx -0.596$ and $\langle P_c \rangle = \langle P_d \rangle = \langle P_e \rangle \approx 0.005$, so that $E \approx -0.895J_1 + 0.015J_2$. Comparing these two energies may serve as a rough estimate and we learn that tetramerization becomes favorable for $J_2 \gtrsim 1.6J_1$. To get a better estimate of the transition, we searched for the minimum energy as we increased the J_2, using the tabulated values of the exchange expectation for different values of t_{tet} and ε_{tet}. In this approach, the transition takes place at $J_2 \approx 0.38J_1$, as seen in Fig. 8. The two minima in the energy-order parameter plot (the inset in Fig. 8) are much less pronounced than in the case when the tetramerization was induced by the four-spin term Q (see the corresponding inset in Fig. 7), and, as a consequence, the first order character of the phase transition is weaker.

In the case of very strong J_2/J_1 (*i.e.* $J_1 \to 0$), we get two decoupled triangular lattices. The SU(4) problem on the triangular lattice was studied in Ref. [34], where a plaquette state of resonating SU(4) singlets is proposed as the ground state, with a large (12 site) unit cell. Thus we may expect another phase transition, as the J_2/J_1 is increased.

V. CONCLUSIONS

We studied the tetramerized ground state of the SU(4) Heisenberg model on the honeycomb lattice. First, we showed that by adding four-site terms of the form $P_{ij}P_{kl}$ to the Hamiltonian, one can construct a model where the product of four-site SU(4) singlets is an exact ground state. This ground state breaks the translational invariance and is four-fold degenerate. To characterize the tetramerization, we constructed an order parameter.

Next, we built a free-fermion Hamiltonian with a π-flux and hopping amplitudes t_{tet} and on-site energies ε_{tet} that is compatible with the tetramerization pattern. The Gutzwiller projected quarter filled Fermi-sea of this Hamiltonian is capable of interpolating between the algebraic color liquid of the pure Heisenberg model and the tetramer-product wave function of the exact ground state for the Hamiltonian with the four-site term.

Using a variational Monte-Carlo method to evaluate the Gutzwiller projected fermionic wave function, we calculated the energy of the Heisenberg model with the nearest neighbor exchange for different values of the hopping parameters t_{tet} and on-site energies ε_{tet} that controlled the degree of tetramerizaton. In the band structure of the free fermions a Dirac point is formed for a particular combination of the t_{tet} and ε_{tet}. The energy is minimal along an extended valley in the $(t_{\text{tet}}, \varepsilon_{\text{tet}})$ plane that closely follows the line of the formation of the Dirac point, together with a vanishing tetramerization, showing the significance of having a Fermi-point instead of a gapped spectrum. Actually, when we plotted the expectation values of the exchanges against each other, they roughly fell on single lines.

The algebraic color-liquid extends in a finite region around the nearest neighbor model, and there is a first order phase transition between the tetramerized state and the algebraic color-liquid as we decreased the strength of the four-site terms. Finally, we looked at the effect of the second neighbor exchange. Within the Variational Monte Carlo method, the algebraic color liquid is the ground state for $J_2 \lesssim 0.38J_1$, and the tetramerized state will have lower energy $J_2 \gtrsim 0.38J_1$.

ACKNOWLEDGMENTS

The authors thank P. Corboz, A. M. Läuchli, F. Mila, and G.Szirmai for stimulating discussions. We are grateful for the support of the Hungarian OTKA Grant No. 106047.

[1] Y. Kitaoka, T. Kobayashi, A. Kōda, H. Wakabayashi, Y. Nino, H. Yamakage, S. Taguchi, K. Amaya, K. Yamaura, M. Takano, A. Hirano, and R. Kanno, J. Phys. Soc. Jpn. **67**, 3703 (1998).
[2] F. Reynaud, D. Mertz, F. Celestini, J. Debierre, A. M. Ghorayeb, P. Simon, A. Stepanov, J. Voiron, and C. Delmas, Phys. Rev. Lett. **86**, 3638 (2001).
[3] S. Nakatsuji, K. Kuga, K. Kimura, R. Satake, N. Katayama, E. Nishibori, H. Sawa, R. Ishii, M. Hagiwara, F. Bridges, T. U. Ito, W. Higemoto, Y. Karaki, M. Halim, A. A. Nugroho, J. A. Rodriguez-Rivera, M. A. Green, and C. Broholm, Science **336**, 559 (2012).

[4] J. A. Quilliam, F. Bert, E. Kermarrec, C. Payen, C. Guillot-Deudon, P. Bonville, C. Baines, H. Luetkens, and P. Mendels, Phys. Rev. Lett. **109**, 117203 (2012).
[5] S. Ishihara, M. Yamanaka, and N. Nagaosa, Phys. Rev. B **56**, 686 (1997).
[6] L. F. Feiner, A. M. Oleś, and J. Zaanen, Phys. Rev. Lett. **78**, 2799 (1997).
[7] Y. Q. Li, M. Ma, D. N. Shi, and F. C. Zhang, Phys. Rev. Lett. **81**, 3527 (1998).
[8] G. Khaliullin and S. Maekawa, Phys. Rev. Lett. **85**, 3950 (2000).
[9] F. Vernay, K. Penc, P. Fazekas, and F. Mila, Phys. Rev. B **70**, 014428 (2004).
[10] F. Wang and A. Vishwanath, Phys. Rev. B **80**, 064413 (2009).
[11] J. Chaloupka and A. M. Oleś, Phys. Rev. B **83**, 094406 (2011).
[12] J. Nasu and S. Ishihara, ArXiv e-prints (2012), arXiv:1209.0239 [cond-mat.str-el].
[13] C. Wu, J.-P. Hu, and S.-C. Zhang, Phys. Rev. Lett. **91**, 186402 (2003).
[14] C. Honerkamp and W. Hofstetter, Phys. Rev. Lett. **92**, 170403 (2004).
[15] M. A. Cazalilla, A. F. Ho, and M. Ueda, New J. Phys. **11**, 103033 (2009).
[16] A. V. Gorshkov, M. Hermele, V. Gurarie, C. Xu, P. S. Julienne, J. Ye, P. Zoller, E. Demler, M. D. Lukin, and A. M. Rey, Nat Phys **6**, 289 (2010).
[17] P. Corboz, M. Lajkó, A. M. Läuchli, K. Penc, and F. Mila, Phys. Rev. X **2**, 041013 (2012).
[18] M. van den Bossche, P. Azaria, P. Lecheminant, and F. Mila, Phys. Rev. Lett. **86**, 4124 (2001).
[19] S. Chen, C. Wu, S.-C. Zhang, and Y. Wang, Phys. Rev. B **72**, 214428 (2005).
[20] P. Corboz, K. Penc, F. Mila, and A. M. Läuchli, Phys. Rev. B **86**, 041106 (2012).
[21] M. van den Bossche, F.-C. Zhang, and F. Mila, The European Physical Journal B - Condensed Matter and Complex Systems
[22] E. Szirmai and M. Lewenstein, EPL (Europhysics Letters) **93**, 66005 (2011).
[23] H.-H. Hung, Y. Wang, and C. Wu, Phys. Rev. B **84**, 054406 (2011).
[24] P. Corboz, A. M. Läuchli, K. Penc, M. Troyer, and F. Mila, Phys. Rev. Lett. **107**, 215301 (2011).
[25] D. P. Arovas, Phys. Rev. B **77**, 104404 (2008).
[26] M. Greiter and S. Rachel, Phys. Rev. B **75**, 184441 (2007).
[27] I. Affleck and J. B. Marston, Phys. Rev. B **37**, 3774 (1988).
[28] M. Hermele, V. Gurarie, and A. M. Rey, Phys. Rev. Lett. **103**, 135301 (2009).
[29] G. Szirmai, E. Szirmai, A. Zamora, and M. Lewenstein, Phys. Rev. A **84**, 011611 (2011).
[30] H. Yokoyama and H. Shiba, J. Phys. Soc. Jpn. **56**, 1490 (1987).
[31] C. Gros, Annals of Physics **189**, 53 (1989).
[32] S. Bieri, M. Serbyn, T. Senthil, and P. A. Lee, Phys. Rev. B **86**, 224409 (2012).
[33] P. Corboz, M. Lajkó, K. Penc, F. Mila, and A. M. Läuchli, ArXiv e-prints (2013), arXiv:1302.1108 [cond-mat.str-el].
[34] K. Penc, M. Mambrini, P. Fazekas, and F. Mila, Phys. Rev. B **68**, 012408 (2003).